Improving approach-avoidance control in social anxiety by targeting phase-amplitude coupling between prefrontal and sensorimotor cortex

Sjoerd Meijer[1,*], Bob Bramson[1,2,*], Ivan Toni[1,†], and Karin Roelofs[1,2,†]

[1]Donders Institute for Brain, Cognition and Behavior, Centre for Cognitive Neuroimaging (DCCN), Radboud University Nijmegen, 6525 EN Nijmegen, the Netherlands.
[2]Behavioral Science Institute (BSI), Radboud University Nijmegen, 6525 GD Nijmegen, the Netherlands.

[*,†]These authors contributed equally.

Keywords: emotional action control, prefrontal control, approach-avoidance, anxiety, dorsolateral prefrontal cortex, transcranial alternating current stimulation, phase-amplitude coupling, oscillations.

Conflict of interest: no competing interests to declare.

Acknowledgments: This work was funded by a consolidator grant DARE2APPROACH, from the European Research Council (ERC_CoG_772337) awarded to KR and also supporting SM and BB; by a consortium grant from the Dutch Research Council INTENSE (NWO_Crossover_17619) and by (NWO_SSH_406.20.GO.020) awarded to IT and KR.

Correspondence:

Sjoerd Meijer
E-mail: sjoerd.meijer@donders.ru.nl
Donders Centre for Cognitive Neuroimaging (DCCN)
Radboud University Nijmegen
Trigon Building
Kapittelweg 29
6525 EN Nijmegen
the Netherlands

Abstract

Avoidance behavior is a major causal and maintaining factor in anxiety. As anxious individuals avoid social situations, their fear cannot be extinguished and context-appropriate behavior cannot be learned. It has been shown that successful emotion control over social approach-avoidance actions relies on theta-gamma phase-amplitude coupling between the lateral prefrontal cortex (lPFC) and the sensorimotor cortices (SMC). Emotional action control can also be facilitated by targeting theta-gamma phase-amplitude coupling between lPFC and SMC using dual-site transcranial alternating current stimulation (dual-tACS), in non-anxious individuals (Bramson et al., 2020). However, it remains unclear whether this intervention is effective where it is needed: For instance, socially anxious individuals fail to recruit lPFC and rely on the dorsolateral prefrontal cortex (dlPFC) for emotional action control (Bramson et al., 2023). Here, we show that dual-tACS improves emotional action control in social anxiety, acting on dlPFC-SMC coupling instead of lPFC-SMC coupling. Forty-nine highly socially anxious individuals performed a social approach-avoidance task while receiving dual-site in-phase, anti-phase, and sham tACS. Concurrent BOLD fMRI measurements revealed that the neural response to tACS in dlPFC mediates improvement in emotional action control induced by the in-phase stimulation. Notably, the extent of dlPFC engagement scaled to individuals' trait anxiety levels. These findings illustrate how human neurophysiological connectivity can be leveraged to improve emotion control over social avoidance, opening the way for mechanistically-grounded clinical interventions of persistent avoidance in anxiety disorders.

Introduction

Anxiety disorders are marked by an inability to flexibly regulate prepotent approach and avoidance tendencies to adapt behavior to contextual demands. Persistent avoidance of perceived threats is shown to cause and maintain anxiety and prevent learning through threat exposure, thereby exacerbating the disorder (Craske & Stein, 2016). Developing effective interventions to improve emotion control in anxious individuals is challenging, partly due to the complexities of translating mechanistic knowledge of brain functions to effective interventions. However, recent work offers promise in improving cognitive and behavioral functions by utilizing dual-site phase-amplitude-coupled transcranial alternating current stimulation (dual-tACS) (Grover et al., 2022; Polanía et al., 2012; Preisig et al., 2021; Reinhart & Nguyen, 2019; Violante et al., 2017). This non-invasive neuromodulation technique can enhance emotion control in non-anxious individuals (Bramson et al., 2020). Here, we test the generalizability of this approach by applying dual-tACS in a group of participants selected for high social anxiety, a trait known to be associated with impaired emotional action control (Heuer et al., 2007; Roelofs, van Peer, et al., 2009; van Peer et al., 2009). This translational test is a critical step toward developing novel clinical interventions directly targeting the underlying neural circuit mechanisms responsible for impaired emotional behavioral control.

Patients suffering from social anxiety disorder have particular difficulties in overriding automatic avoidance tendencies in social situations. Previous research has identified the lateral prefrontal cortex (lPFC) as a critical brain region involved in selecting competing approach-avoidance actions (Badre, 2008; Boorman et al., 2011; Voytek et al., 2015). This control is implemented through rhythmic modulation of activity in downstream areas, including the sensorimotor cortex (SMC) and parietal cortex (Bramson et al., 2018, 2020; Canolty & Knight, 2010; Voytek et al., 2015). Specifically, successful control over social-emotional approach-avoidance actions has been linked to temporal coupling between the phase of theta-band rhythms in lPFC and the amplitude of gamma-band activity in SMC (Bramson et al., 2018; Voytek et al., 2015). Dual-tACS offers a means to non-invasively modulate inter-regional phase-amplitude coupling in humans, enhancing long-range synchronization between task-relevant neural circuits (Bramson et al., 2020; Grover et al., 2022; Reinhart & Nguyen, 2019). Recent applications of dual-tACS have successfully improved emotional action

control in non-anxious participants. In-phase stimulation, designed to synchronize peaks of theta-band rhythms in lPFC with the amplitude of gamma-band neural activity in SMC, led to significantly fewer errors when participants had to override automatic emotional action tendencies (Bramson et al., 2020). Given the pivotal role of the lPFC in regulating approach-avoidance actions (Volman et al., 2011) and the importance of theta-gamma coupling between lPFC and SMC for successful control over social-emotional approach-avoidance actions (Bramson et al., 2018, 2020), our investigation aims to test whether dual-tACS applied to lPFC-SMC can similarly enhance behavioral outcomes in highly socially anxious individuals.

In this study, we applied the dual-tACS intervention to a group of forty-nine highly socially anxious individuals. We exposed them to an approach-avoidance fMRI task during dual-tACS intervention, similar to the methodology used in our previous study with non-anxious male participants (Bramson et al., 2020). Given that high-anxious participants vary in their use of prefrontal resources to implement control over emotional action tendencies (Bramson et al., 2023), we also measured concurrent fMRI during task performance under dual-tACS to assess prefrontal engagement to dual-tACS.

Results

Emotional action control: Behavioral performance and neural activation

Participants, selected on high self-reported social anxiety (Figure 1a), were instructed to use a joystick to approach happy and avoid angry faces (affect-congruent condition) or avoid happy and approach angry faces (affect-incongruent condition; Figure 1b). The affect-incongruent condition requires participants to override automatic emotional action tendencies to avoid angry and approach happy faces (Phaf et al., 2014; Roelofs, Minelli, et al., 2009). In the baseline sham-tACS condition, expected affective congruency effects were observed, with higher error rates for incongruent as compared to congruent responses, b = .41; 95% CI [.22 .61] (Bramson et al., 2018, 2020; Kaldewaij et al., 2021; Volman et al., 2011), Figure 1c. Effects from Bayesian Mixed Effects models were considered significant if the 95% Credible Interval (CI) did not include 0.

The patterns of neural activity largely aligned with previous findings using the same task, showing increased activation during incongruent *versus* congruent trials in bilateral parietal cortex, precuneus, and right dorsal anterior cingulate cortex, as well as decreased activity in bilateral medial and orbitofrontal cortex, parahippocampal gyrus, amygdala-hippocampus, temporal pole, and right fusiform cortex (Bramson *et al*., 2020; Bramson *et al.* 2018; Volman *et al*., 2011), Figure 1d. However, highly anxious individuals exhibited more robust activation for incongruent trials in the dorsolateral prefrontal cortex (dlPFC) [30, 36, 38], rather than in the lPFC region previously found in non-anxious individuals (Kaldewaij *et al.*, 2021; Bramson *et al.*, 2020; Lapate *et al.* 2022). The differences in emotional action control circuits between high-anxious and non-anxious individuals have been detailed in a separate paper (Bramson et al., 2023). These findings indicate that high-anxious and non-anxious individuals show similar behavioral difficulties in controlling emotional action tendencies. Still, high-anxious individuals likely implement control using dlPFC rather than lPFC (Bramson et al., 2023).

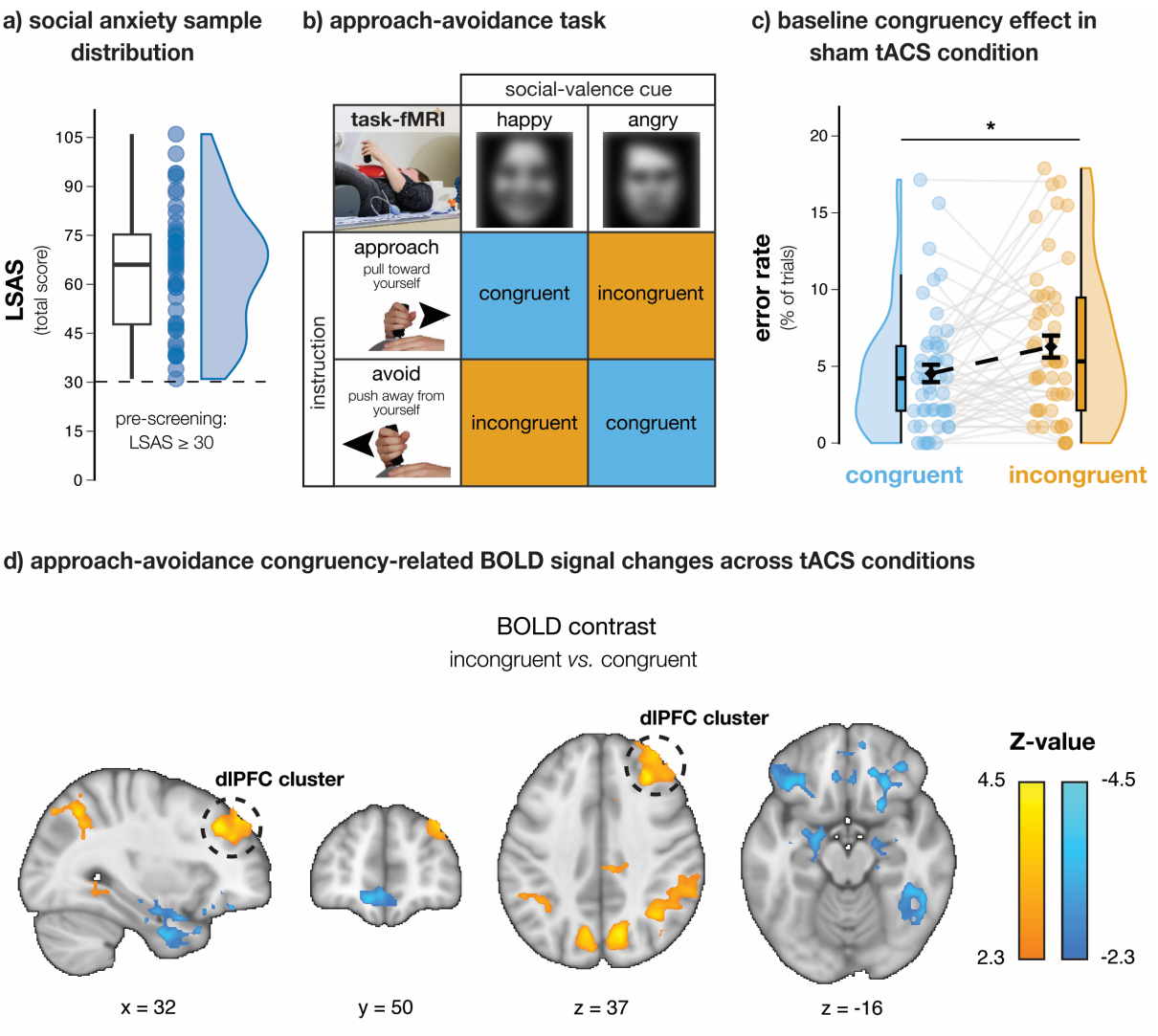

Figure 1. Behavioral and BOLD fMRI effects related to control over emotional action tendencies.

(a) Sample distribution of self-reported Liebowitz Social Anxiety Scale (LSAS) scores. The black dashed line marks an LSAS score of 30, used to select socially anxious participants. This cut-off balances specificity and sensitivity in detecting social anxiety (Mennin et al., 2002). (b) Conceptual visualization of the approach-avoidance task performed during concurrent dual-tACS fMRI. In affect-congruent conditions, participants were instructed to pull the joystick towards them in response to a happy face and push it away from them in response to an angry face. In contrast, the affect-incongruent condition requires participants to override automatic emotional action tendencies to avoid angry and approach happy faces. Therefore, in this condition, participants were instructed to pull the joystick towards them in response to an angry face and push it away in response to a happy face. (c) Behavioral congruency-effects

in the baseline sham stimulation condition of the task. Participants made more errors when overriding their automatic emotional action tendencies in the affect-incongruent condition (orange circles) as compared to making affect-congruent responses (blue circles), b = .41; 95% CI [.22 .61]. Black-filled diamonds represent mean values, and standard errors of the mean are shown with black lines. (d) Task-fMRI congruency-related effects across tACS stimulation conditions (incongruent > congruent; cluster-level inferences corrected for multiple comparisons). Stronger BOLD signals were observed in prefrontal- and parietal areas when automatic emotional action tendencies needed to be overridden, while amygdala-hippocampal and medial-orbitofrontal areas showed weaker BOLD signals.

tACS dose- and phase-dependent modulation of emotional action control

Transcranial current stimulation, when effective, modulates ongoing neural activity (Feurra et al., 2013; Ruhnau et al., 2016). Following our pre-registered analysis pipeline (https://osf.io/j9s2z), we evaluated the cerebral effects of prefrontal tACS by examining BOLD activity in the region involved in implementing emotional action control in these high-anxious participants. High-anxious individuals recruit dlPFC rather than lPFC to solve emotional action control (Bramson et al., 2023). Additionally, the distribution of the current evoked by the dual-tACS montage of this study includes dlPFC (Figure 2a). Therefore, we chose BOLD activity over dlPFC as a metric of tACS dose-response. Similar to our previous study (Bramson et al., 2020), the tACS-dose metric is obtained from a BOLD contrast (active tACS > sham tACS) that is orthogonal to both the tACS phase manipulation (Figure 2b) and the emotional action control contrast. Critically, we observe tACS-dose and tACS-phase specific enhancement of emotional action control, b = -.35; 95% CI [-.67 -.03] ([emotional action control * tACS-phase * tACS-dose dlPFC]) (Figure 2c). Participants with a stronger dlPFC dose-response to tACS also exhibited greater improvement in controlling their emotional actions when receiving in-phase as opposed to anti-phase tACS. Planned post-hoc analyses confirm significant dose-dependent effects for the in-phase (Spearman's $\rho(47) = -0.37$, $p = .009$) but not for the anti-phase condition (Spearman's $\rho(47) = 0.09$, $p = .519$). The direction and magnitude of the dual-tACS intervention effects align with

our previous report (Bramson et al., 2020). Accordingly, when extracting tACS-dose from lPFC, a region previously reported to be decoupled from emotional action control in high-anxious individuals (Bramson et al., 2023), no significant tACS-induced changes in emotional action control were observed (*b* = -.12; 95% CI [-.45 .23] ([emotional action control * tACS-phase * tACS-dose lPFC]). Moreover, further exploration of brain-symptoms correlations revealed a positive association between higher trait anxiety levels and stronger tACS-dose in dlPFC (Figure 2d). These findings demonstrate that dual-tACS can effectively enhance emotional action control in high-anxious individuals by improving phase-amplitude coupling between dlPFC and SMC.

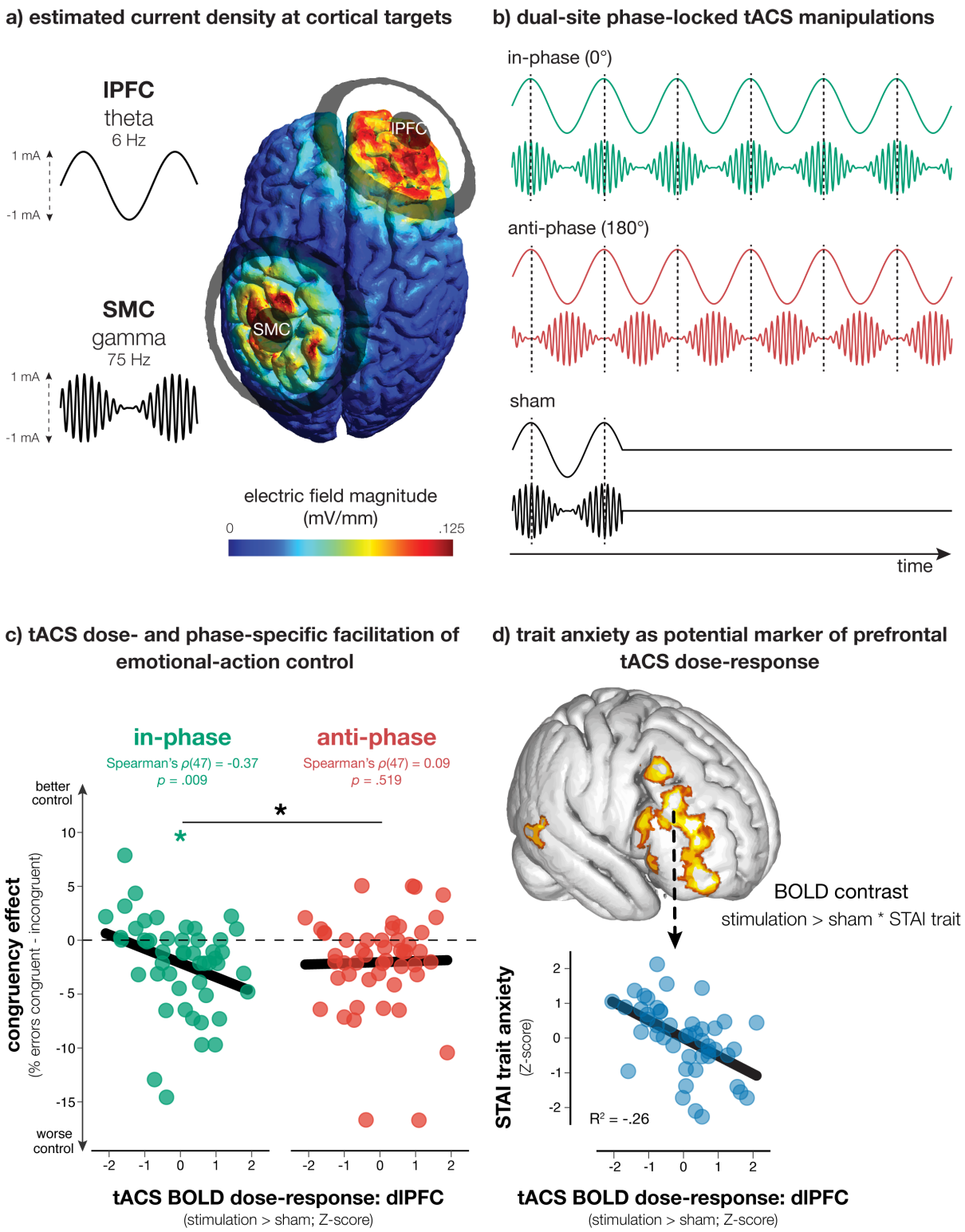

Figure 2. Dose- and phase-specific effects of dual-site lPFC-SMC theta-gamma phase-amplitude coupled tACS on emotional action control in social anxiety. *(a) Two sets of concentric ring electrodes were placed over the right lPFC and left SMC. The current density model shows the spatial distribution of the electric field*

*magnitude (mV/mm) evoked by the high-definition montage at both cortical targets, with intensities that can influence endogenous task-evoked oscillatory activity. (b) The stimulation conditions underwent a pseudo-random alternation throughout the experiment between in-phase, anti-phase, and sham conditions. Specifically, 75 Hz stimulation was administered over the SMC and its amplitude modulated by 6 Hz stimulation over the lPFC. Modulation was either in-phase or anti-phase with the peaks of the 6 Hz lPFC stimulation. The sham condition involved a brief 10-second initial stimulation that was discontinued before the start of the first trial. (c) Participants showing more robust inhibitory responses to theta-band stimulation over dlPFC, evidenced by a decrease in blood-oxygen-level-dependent (BOLD) signal (Bramson et al., 2020; Scheeringa et al., 2011), exhibited improved control over emotional actions (i.e., decreased congruency effect) during in-phase dual-tACS (in green) compared to anti-phase dual-tACS (in red), b = -.35; 95% CI [-.67 -.03] ([emotional action control (congruent, incongruent) * tACS-phase (in-phase, anti-phase) * tACS-dose dlPFC])*. *(d) Concurrent tACS-fMRI BOLD signal changes across in-phase and anti-phase tACS stimulation conditions correlated with trait anxiety, showing stronger dlPFC dose-response for individuals with higher trait anxiety levels.*

Discussion

This study demonstrates that in-phase dual-tACS, targeted at facilitating endogenous theta-gamma phase-amplitude coupling between lPFC and SMC, enhances control over emotional action tendencies in highly socially anxious individuals. The main finding is that dual-tACS effects, previously reported to improve control over automatic approach-avoidance tendencies in non-anxious participants (Bramson et al., 2020), can also generalize to a clinically relevant population with altered control over daily-life social-emotional behavior (Roelofs, van Peer, et al., 2009; van Peer et al., 2009). Furthermore, this study shows that the dual-tACS effect in high-anxious males and females modulates a different prefrontal territory (dlPFC) than in non-anxious males (lPFC; Bramson et al., 2020). This observation fits with the recently reported shift in the prefrontal circuit implementing emotional action control from lPFC (non-anxious participants) to dlPFC (high-anxious participants) (Bramson et al., 2023). The current study demonstrates the possibility of improving emotional action control using dual-tACS in high-anxious individuals via facilitation of endogenous long-range phase-amplitude coupling. This finding extends our mechanistic understanding of approach-avoidance control in social anxiety and introduces phase-amplitude coupling between dlPFC and SMC as a novel therapeutic target.

dlPFC-SMC phase-amplitude coupling supports emotional action control in social anxiety

This dual-tACS intervention builds on prior studies that have demonstrated the significance of endogenous lPFC-SMC theta-gamma coupling in controlling automatic emotional action tendencies and in facilitating the implementation of alternative goal-directed actions (Bramson et al., 2018, 2020). In-phase dual-tACS can facilitate dlPFC-SMC coupling, promoting interregional synchronization of neuronal excitability periods and supporting valence-incongruent action goals in dlPFC to bias action selection in SMC (Bramson et al., 2018; Voytek et al., 2015). In one important detail, this putative mechanism differs from what has been observed in healthy individuals. In healthy individuals, prefrontal control emerged from lPFC (Bramson et al., 2020) rather than dlPFC (this study). lPFC is a region that can flexibly integrate valence

signals with approach-avoid action selection, allowing lPFC to orchestrate goal-directed control over automatic emotional action tendencies (Bramson et al., 2019; Lapate et al., 2022). Unfortunately, the lPFC is overexcitable in high-anxious individuals (Bramson et al., 2023), likely reducing its ability to discriminate between afferent emotional valence signals. We have previously suggested that, in high-anxious individuals, the dlPFC might compensate for lPFC when control over emotional actions is required, in the context of mild emotional challenges, such as the approach-avoidance task. In contrast with integrated valence-action goal representations in lPFC, action goal representations in dlPFC are not modulated by valence (Lapate et al., 2022). This is likely due to its relatively limited mono-synaptic connections with the amygdala complex (compared to human lPFC) (Folloni et al., 2019; Petrides & Pandya, 1999). Thus, the dlPFC can implement rule-based actions with minimal interference from emotional valence signals even in high anxiety, when emotional signals would saturate an already overexcitable lPFC (Bramson et al., 2023). However, dlPFC-based emotional control might be less successful in real-life situations, when emotional challenges co-occur with other demands for cognitive control. In support of this interpretation, emotional working memory training successfully reduced the impact of emotional context on behavioral performance (Schweizer et al., 2013). We extend these findings using a circuit-level approach to directly target and improve emotional action control.

tACS BOLD dose-response in dlPFC scales with trait anxiety

The current study has shown that the application of in-phase dual-tACS results in behavioral effects proportional to the dlPFC BOLD signal evoked by the prefrontal tACS electrode, i.e. a dose-response effect. This finding corresponds to the observation that high-anxious individuals recruit the dlPFC when instructed to control automatic emotional action tendencies (Bramson et al., 2023). We also observe that individuals with higher trait anxiety exhibit more robust dlPFC responses to the tACS intervention. This finding corresponds to the observation that trait anxiety is associated with an anatomical shift of prefrontal emotional action control, from lPFC to dlPFC (Bramson et al., 2023). Given that in-phase dual-tACS is expected to reduce noise within a hypo-synchronized circuit supporting task performance (Wischnewski et al.,

2023), we predict that trait anxiety might also index individual levels of neural noise within the dlPFC-SMC circuit during emotional action control. This prediction could be tested by measuring electrophysiological activity during emotional action control in high-anxious individuals (Bramson et al., 2018), confirming further the notion that trait anxiety predicts individual variation in response to tACS. This is important because using trait anxiety facilitates the translation of dual-tACS to clinical protocols, without the need to estimate tACS response using concurrent fMRI.

Considerations and future directions

It could be argued that the current findings are limited by the lack of direct observations on tACS-induced rhythmic entrainment. In fact, the manipulation of dual-tACS phase angle (in-phase *versus* anti-phase) enables us to relate the tACS effects to phase-specific changes in long-range phase-amplitude coupling, and exclude general changes in lPFC or SMC excitability. The phase manipulation provides the additional benefit of fully matching peripheral effects between in-phase and anti-phase stimulation, thereby ruling out alternative explanations related to transcutaneous entrainment or retinal stimulation (Asamoah et al., 2019; Schutter, 2016).

In this study, phase-specific dual-tACS improvements in emotional action control are dose-specific, which suggests high inter-individual variation in the effects of dual-tACS on emotion control. This signals the need to identify factors that predict inter-individual variation in intervention response, e.g. what percentage of individuals respond to the intervention. For this reason, we also consider clinically relevant person-centered effect sizes, showing that over half of the participants (55%) presented the expected pattern of error rates for in-phase dual-tACS as compared to sham tACS (Grice et al., 2020). We consider this intervention response percentage promising. Although our task only poses a mild emotional challenge, as reflected in low baseline sham error rates, performance was nonetheless improved, with a group-average 13% reduction in error rates comparing in-phase to sham stimulation. Furthermore, it is important to note that the dual-tACS intervention is not intended to be a standalone treatment, but rather to enhance the effectiveness of existing treatments. This can include improving the ability to control emotional behavior during exposure therapy to confront threatening situations and temporarily interrupt the cycle

of persistent avoidance. Hence, studying how existing treatments interact with our neuromodulation intervention in clinical settings is essential.

Conclusion

Building non-invasive neuromodulation interventions that facilitate a cognitive function presents a major neuroscientific challenge, due to the requirement to identify and enhance the underlying endogenous neural dynamics. Translating mechanistically-informed neuromodulation interventions from healthy individuals to clinical populations poses a further challenge, due to incomplete understanding of the neural mechanisms underlying neural disorders. Here, we successfully translate a mechanistically informed dual-tACS intervention (Bramson et al., 2018, 2020) to a clinically relevant high-anxiety population that shows impairments in daily-life social-emotional behavior. The findings highlight the advantage of combining cognitive neuromodulation interventions with neuroimaging during the early stages of clinical translation. The advantage of this multi-modal approach is to offer a better understanding of the intervention mechanism, leading to more precise characterization of inter-individual variation in intervention response. The results provide insights into the role of phase-amplitude coupling between lPFC and SMC in emotion control over social approach-avoidance behavior and contribute to developing targeted clinical interventions for anxiety.

Methods

Participants

Fifty-two highly socially anxious students (39 females) from Radboud University, Nijmegen, were recruited to participate in this pre-registered experiment (https://osf.io/j9s2z). The local ethics committee approved the experiment (METC Arnhem-Nijmegen: CMO2014/288). We had to exclude 3 participants due to technical issues. Participants were selected based on high self-reported social anxiety levels, as detailed below, and screened on eligibility criteria, including no history of mental illness or use of psychoactive medication. Additionally, we confirmed that participants had normal or corrected-to-normal vision and underwent screening for contraindications to magnetic resonance imaging (MRI) and non-invasive transcranial electrical stimulation. The mean age of the participants was 24.0 years, with an SD of ±4.3, and a range of 19 to 40.

Pre-screening took place using the Liebowitz Social Anxiety Scale (LSAS). Participants scoring 30 or higher (fear/anxiety and avoidance sub-scales combined) were included as this criterion provides an optimal balance between sensitivity and specificity in identifying individuals who meet the criteria for social anxiety disorder (Mennin et al., 2002). This selection criterion resulted in an approximately normal distribution of LSAS scores within our study sample, with a mean of 64.4, a standard deviation (SD) of ±19.0, and a range from 31 to 106 (Figure 1a). The trait sub-scale of the State-Trait Anxiety Inventory (STAI Y-2) was included to assess trait anxiety as an inter-individual difference marker of tACS BOLD dose-response, as endogenous prefrontal activation to the emotional-action control challenge varies as a function of trait anxiety (Bramson et al., 2023).

The current study in highly socially anxious individuals was designed to replicate the main finding of our previous investigation in healthy male students (Bramson et al., 2020) that showed tACS phase- and dose-specific effects on emotional action control (https://osf.io/j9s2z). This required a sample size that allowed us to detect the previously observed significant three-way interaction between Congruency (congruent, incongruent) * Stimulation (in-phase, anti-phase) * tACS-dose (BOLD signal in lPFC during stimulation *vs*. sham): $\eta_p^2 = 0.19$ (Bramson et al.,

2020). The minimum sample size required for this study to detect an effect of comparable magnitude is 45 participants (*a priori* sensitivity power analysis of RM-ANCOVA: α = .05, power = .80, η_p^2 = 0.19; G*Power v3.1; Faul et al., 2007). Given that the current sample might be more heterogeneous due to mixed-sex and anxiety-related differences, and the precision of effect size estimates show regression towards the mean (Bramson et al., 2020), we decided to increase our planned sample size to 50 participants.

Procedure

The data collection procedure spanned three separate days. On the first day, participants completed the Liebowitz Social Anxiety Scale (LSAS) and State-Trait Anxiety Inventory-Trait (STAI-trait, Y-2) questionnaires. Following this, participants underwent various scanning procedures, including a structural T1-weighted scan, a diffusion-weighted imaging scan (DWI, as reported in Bramson et al., 2023), and a magnetic spectroscopy scan (MRS, as reported in Bramson et al., 2023).

During the second and third days, neuronavigation was used to position the electrodes over the sensorimotor cortex (SMC) and prefrontal cortex (lPFC). For details regarding electrode placement, please refer to the subsequent section. Subsequently, during both stimulation sessions, participants were inside the MR scanner. They performed a 5-minute practice task before proceeding to complete the approach-avoidance task with concurrent dual-tACS and task-based functional MRI for approximately 35 minutes.

Approach-avoidance task

Emotional action control was manipulated using a validated social approach-avoidance task in which cognitive control is associated with lPFC-SMC theta-gamma coupling (Bramson et al., 2018), and is sensitive to the phase-dependent effects of dual-site theta-gamma phase-amplitude tACS when controlling for inter-individual variation in prefrontal BOLD response to tACS (Bramson et al., 2020). During functional MR scanning, participants lay inside the MR scanner with a joystick in their right hand resting on their lower abdomen. Participants were instructed to approach or avoid by moving the joystick toward or away from themselves, respectively. During

the task, participants received written instructions on the screen (> 10 s) at the start of each block of 12 trials (~60 s) that stated, “Pull the joystick toward yourself when you see a happy face and push away from yourself when you see an angry face” (congruent condition), “Push the joystick away from yourself when you see a happy face and pull toward yourself when you see an angry face” (incongruent condition). Congruent and incongruent conditions alternated between blocks in a pseudo-random fashion. Between blocks, there was an inter-block interval of > 20 s. Each trial started with a fixation cross (500 ms) followed by a face stimulus (100 ms) to which participants had to respond within 2 s. Joystick movements over 30% of the maximum movement range were considered valid responses. If a participant did not respond, they would receive on-screen feedback stating, "You did not move the joystick far enough". Instructions and the inter-block interval lead to an ~30 s wash-out period between stimulation conditions. Each participant had 288 trials on each of the two testing days, yielding 576 observations (trials) in total, equally distributed over congruency (congruent, incongruent) and stimulation (in-phase, anti-phase, sham) condition combinations (96 trials per bin).

Dual-tACS

Transcranial alternating current stimulation (tACS) was applied online during task performance inside the MRI scanner using two sets of concentric ring electrodes (inner disc: 25 mm ø; outer ring: 80 mm inner-ø, 100 mm outer-ø) (Saturnino et al., 2017). Current direction alternated (-1 mA to +1 mA) between each disc-ring electrode set to achieve a time-varying electrical field in theta-band (6 Hz) frequency over right-lPFC and gamma-band (75 Hz) tapered with a 6 Hz theta wave over left-SMC. The tACS-phase manipulation was achieved by phase-locking gamma-band power to peaks (in-phase) or troughs (anti-phase) of the theta-band signal. During sham blocks, there was an initial 10 s period of stimulation to match potential sensations related to the onset of stimulation, after which stimulation was terminated. Within a session, participants received all stimulation conditions (in-phase, anti-phase, sham) alternating in a pseudo-random fashion between stimulus blocks of 12 trials (~60 s), interleaved with periods of no stimulation (instructions between blocks; > 30 s), and never repeating the same stimulation condition for two consecutive blocks.

We used neuronavigation (Localite TMS Navigator; https://www.localite.de/en/products/tms-navigator/; RRID: SCR_016126) for individualized targeting of left-SMC (MNI [-28, -32, 64]; Bramson et al., 2018, 2020) and right-lPFC (MNI [26, 54, 0]; Bramson et al., 2018, 2020; Neubert et al., 2014) based on anatomical masks of regions of interest registered to individual T1-weighted scans acquired during the first session. After localization, electrodes were attached to the participant's scalp using Ten20 conductive paste (MedCat; https://shop.medcat.nl/Ten20-Pasta-Topf-4-Oz,-3er-Set?Product=256922614&Lng=en). Inside the MR scanner, stimulation was delivered using two Neuroconn DC-PLUS stimulators (impedance < 10 kOhm; https://www.neurocaregroup.com/dc_stimulator_plus.html; RRID: SCR_015520). Stimulators were placed inside a magnetically shielded box designed with electronics that filtered out RF pulses of the MR scanner and combined with a BrainAmp ExG MR amplifier (www.brainproducts.com) that allowed continuous monitoring of stimulation output during the session.

Modeling of stimulation currents

The electric field magnitude (mV/mm) at the cortical target sites was estimated using SimNIBS (version 4.0; https://simnibs.github.io/simnibs/build/html/index.html; Thielscher et al., 2015). The concentric ring electrode sets were modeled as the disc (25 mm ø) and outer ring electrode (80 mm inner-ø, 100 mm outer-ø) with the same center, using a 2-layer medium (2 mm silicone rubber on top of 2 mm saline gel). The electrode sets were positioned over lPFC ([38, 95, 60]) and SMC ([-36, -10, 90]) using the template head mesh of SimNIBS. For all media, we used standard conductivities provided by SimNIBS. Direct currents of 1 mA were modeled to flow between the center disc electrode and the outer ring. The model results of the electric field magnitude at the cortical surface for both target sites are shown in Figure 2a.

Behavior analyses

To determine the phase-dependent effect of tACS on emotional action control, error rates were compared between congruent and incongruent trials while controlling for dose-dependent effects of tACS ('tACS-dose'). This three-way interaction (emotional

action control * tACS-phase * tACS-dose) was assessed on congruency effects (congruent *vs.* incongruent) estimated from trial-by-trial responses through Bayesian mixed effects models using the *brms* package (Bürkner, 2017) implemented in the R (https://www.r-project.org/). Bayesian mixed effects models adhered to the maximum random effects structure by including random slopes, intercepts, and correlations that could vary across participants for all fixed effects (congruency- and stimulation conditions). Outputs of these models are log odds with credible intervals ('*B*'). The significance of effects is interpreted based on the credible intervals not including zero in the 95% confidence interval.

We hypothesized that the congruency effect in error rates would decrease for in-phase and increase for anti-phase stimulation and that the size of the effect per participant would depend on the BOLD effect of tACS *versus* sham, a measure of dose dependence that is orthogonal to the contrast of interest (in-phase *versus* anti-phase). These expectations were preregistered at the Open Science Framework: (https://osf.io/j9s2z).

Materials and apparatus

All participants underwent magnetic resonance imaging using a 3T MAGNETROM Prisma MR scanner (Siemens AG, Healthcare Sector, Erlangen, Germany) using a 64-channel head coil with a top opening that allowed the electrode wires to be routed out of the back of the scanner bore.

The scans obtained during the MR sessions were aligned with a standard brain atlas to guarantee a uniform field of view (FoV) throughout the days. Each scanning day involved taking around 1800 functional images using a multi-band 6 sequence, 2 mm isotropic voxel size, TR/TE = 1000 / 34 ms, flip angle = 60°, phase angle P >> A, including ten volumes with reversed phase encoding direction (A >> P) used to correct image distortions.

High-resolution structural images were acquired with a single-shot MPRAGE sequence using a GRAPPA acceleration factor of 2, TR/TE = 2400/2.13 ms, effective voxel size of 1 mm isotropic, 176 sagittal slices, distance factor of 50%, flip angle = 8°, orientation A >> P, FoV = 256 mm.

fMRI analyses – data preprocessing

All processing of the images was performed using MELODIC 3.00 as implemented in FSL 6.0.0 (https://fsl.fmrib.ox.ac.uk; Jenkinson et al., 2012). Images were motion-corrected using MCFLIRT (Jenkinson et al., 2002), and distortions in the magnetic field were corrected using TOPUP (Andersson et al., 2003). Functional images were rigid-body registered to the brain-extracted structural image using FLIRT (Jenkinson et al., 2002). Registration to MNI 2 mm standard space was performed using the nonlinear registration tool FNIRT. Images were spatially smoothed using a Gaussian 5 mm kernel and high pass filtered with a cut-off that was automatically estimated based on the task structure. Independent component analysis was run with a pre-specified maximum of 100 components (Beckmann & Smith, 2004); these components were manually inspected to remove potential sources of noise (Griffanti et al., 2017).

fMRI analyses – GLM

Emotional action control effects on whole-brain BOLD activation were estimated by contrasting incongruent trials (approach angry and avoid happy) with congruent trials (avoid angry and approach happy) across stimulation conditions (in-phase, anti-phase, sham). tACS effects on the whole-brain BOLD signal were estimated by comparing stimulation (in-phase and anti-phase) to sham across congruency conditions (congruent and incongruent). Individual estimates of prefrontal tACS-dose were extracted from the 98% peak activated voxel inside the Harvard-Oxford MNI-space dlPFC (middle frontal gyrus) mask registered to the individual T1-weighted image. We ran an exploratory analysis using whole-brain correlation between individual variation in STAI trait anxiety (Y-2) and tACS-dose contrast.

First- and second-level GLM analyses were performed in FSL 6.0.5 using FEAT (Woolrich et al., 2001). The first-level model included 12 task regressors: approach angry, approach happy, avoid angry, and avoid happy were modeled separately for each stimulation condition (in-phase, anti-phase, and sham). For each regressor, events covered the time interval from stimulus presentation until the corresponding onset of joystick movement. The following nuisance regressors were included in the GLM as nuisance covariates: estimated head translations and rotations (six

regressors), temporal derivates of those translations and rotations (6 regressors), and global signal time series in white matter and cerebrospinal fluid (two regressors). We used fixed effects analyses implemented in FEAT to combine first-level models of the two separate stimulation sessions (Woolrich et al., 2001). Group-level effects were assessed using FLAME 1 with outlier de-weighting (Eklund et al., 2016), making family-wise error-corrected cluster-level inferences using a cluster-forming threshold of $z > 2.3$. This threshold provides a false error rate of ~5 % when using FSL FLAME 1.

Reference list

Andersson, J. L. R., Skare, S., & Ashburner, J. (2003). How to correct susceptibility distortions in spin-echo echo-planar images: Application to diffusion tensor imaging. *NeuroImage*, *20*(2), 870–888. https://doi.org/10.1016/S1053-8119(03)00336-7

Asamoah, B., Khatoun, A., & Mc Laughlin, M. (2019). TACS motor system effects can be caused by transcutaneous stimulation of peripheral nerves. *Nature Communications*, *10*(1), Article 1. https://doi.org/10.1038/s41467-018-08183-w

Badre, D. (2008). Cognitive control, hierarchy, and the rostro–caudal organization of the frontal lobes. *Trends in Cognitive Sciences*, *12*(5), 193–200. https://doi.org/10.1016/j.tics.2008.02.004

Beckmann, C. F., & Smith, S. M. (2004). Probabilistic independent component analysis for functional magnetic resonance imaging. *IEEE Transactions on Medical Imaging*, *23*(2), 137–152. https://doi.org/10.1109/TMI.2003.822821

Boorman, E. D., Behrens, T. E., & Rushworth, M. F. (2011). Counterfactual Choice and Learning in a Neural Network Centered on Human Lateral Frontopolar Cortex. *PLOS Biology*, *9*(6), e1001093. https://doi.org/10.1371/journal.pbio.1001093

Bramson, B., den Ouden, H. E., Toni, I., & Roelofs, K. (2020). Improving emotional-action control by targeting long-range phase-amplitude neuronal coupling. *ELife*, *9*, e59600. https://doi.org/10.7554/eLife.59600

Bramson, B., Folloni, D., Verhagen, L., Hartogsveld, B., Mars, R. B., Toni, I., & Roelofs, K. (2019). *Human lateral Frontal Pole contributes to control over social-emotional action* (p. 584896). bioRxiv. https://doi.org/10.1101/584896

Bramson, B., Jensen, O., Toni, I., & Roelofs, K. (2018). Cortical Oscillatory Mechanisms Supporting the Control of Human Social–Emotional Actions. *Journal of Neuroscience*, *38*(25), 5739–5749. https://doi.org/10.1523/JNEUROSCI.3382-17.2018

Bramson, B., Meijer, S., van Nuland, A., Toni, I., & Roelofs, K. (2023). Anxious individuals shift emotion control from lateral frontal pole to dorsolateral prefrontal cortex. *Nature Communications*, *14*(1), Article 1. https://doi.org/10.1038/s41467-023-40666-3

Bürkner, P.-C. (2017). brms: An R Package for Bayesian Multilevel Models Using Stan. *Journal of Statistical Software*, *80*, 1–28. https://doi.org/10.18637/jss.v080.i01

Canolty, R. T., & Knight, R. T. (2010). The functional role of cross-frequency coupling. *Trends in Cognitive Sciences*, *14*(11), 506–515. https://doi.org/10.1016/j.tics.2010.09.001

Craske, M. G., & Stein, M. B. (2016). Anxiety. *The Lancet*, *388*(10063), 3048–3059. https://doi.org/10.1016/S0140-6736(16)30381-6

Eklund, A., Nichols, T. E., & Knutsson, H. (2016). Cluster failure: Why fMRI inferences for spatial extent have inflated false-positive rates. *Proceedings of the National Academy of Sciences*, *113*(28), 7900–7905. https://doi.org/10.1073/pnas.1602413113

Faul, F., Erdfelder, E., Lang, A.-G., & Buchner, A. (2007). G*Power 3: A flexible statistical power analysis program for the social, behavioral, and biomedical sciences. *Behavior Research Methods*, *39*(2), 175–191. https://doi.org/10.3758/BF03193146

Feurra, M., Pasqualetti, P., Bianco, G., Santarnecchi, E., Rossi, A., & Rossi, S. (2013). State-Dependent Effects of Transcranial Oscillatory Currents on the Motor System: What You Think Matters. *Journal of Neuroscience*, *33*(44), 17483–17489. https://doi.org/10.1523/JNEUROSCI.1414-13.2013

Folloni, D., Sallet, J., Khrapitchev, A. A., Sibson, N., Verhagen, L., & Mars, R. B. (2019). Dichotomous organization of amygdala/temporal-prefrontal bundles in both humans and monkeys. *ELife*, *8*, e47175. https://doi.org/10.7554/eLife.47175

Grice, J. W., Medellin, E., Jones, I., Horvath, S., McDaniel, H., O'lansen, C., & Baker, M. (2020). Persons as Effect Sizes. *Advances in Methods and Practices in Psychological Science*, *3*(4), 443–455. https://doi.org/10.1177/2515245920922982

Griffanti, L., Douaud, G., Bijsterbosch, J., Evangelisti, S., Alfaro-Almagro, F., Glasser, M. F., Duff, E. P., Fitzgibbon, S., Westphal, R., Carone, D., Beckmann, C. F., & Smith, S. M. (2017). Hand classification of fMRI ICA noise components. *NeuroImage*, *154*, 188–205. https://doi.org/10.1016/j.neuroimage.2016.12.036

Grover, S., Wen, W., Viswanathan, V., Gill, C. T., & Reinhart, R. M. G. (2022). Long-lasting, dissociable improvements in working memory and long-term memory in older adults with repetitive neuromodulation. *Nature Neuroscience*, *25*(9), Article 9. https://doi.org/10.1038/s41593-022-01132-3

Heuer, K., Rinck, M., & Becker, E. S. (2007). Avoidance of emotional facial expressions in social anxiety: The Approach–Avoidance Task. *Behaviour Research and Therapy*, *45*(12), 2990–3001. https://doi.org/10.1016/j.brat.2007.08.010

Jenkinson, M., Bannister, P., Brady, M., & Smith, S. (2002). Improved Optimization for the Robust and Accurate Linear Registration and Motion Correction of Brain Images. *NeuroImage*, *17*(2), 825–841. https://doi.org/10.1006/nimg.2002.1132

Jenkinson, M., Beckmann, C. F., Behrens, T. E. J., Woolrich, M. W., & Smith, S. M. (2012). FSL. *NeuroImage*, *62*(2), 782–790. https://doi.org/10.1016/j.neuroimage.2011.09.015

Kaldewaij, R., Koch, S. B. J., Hashemi, M. M., Zhang, W., Klumpers, F., & Roelofs, K. (2021). Anterior prefrontal brain activity during emotion control predicts resilience to post-traumatic stress symptoms. *Nature Human Behaviour*, *5*(8), Article 8. https://doi.org/10.1038/s41562-021-01055-2

Lapate, R. C., Ballard, I. C., Heckner, M. K., & D'Esposito, M. (2022). Emotional Context Sculpts Action Goal Representations in the Lateral Frontal Pole. *Journal of Neuroscience*, *42*(8), 1529–1541. https://doi.org/10.1523/JNEUROSCI.1522-21.2021

Mennin, D. S., Fresco, D. M., Heimberg, R. G., Schneier, F. R., Davies, S. O., & Liebowitz, M. R. (2002). Screening for social anxiety disorder in the clinical setting: Using the Liebowitz Social Anxiety Scale. *Journal of Anxiety Disorders*, *16*(6), 661–673. https://doi.org/10.1016/s0887-6185(02)00134-2

Neubert, F.-X., Mars, R. B., Thomas, A. G., Sallet, J., & Rushworth, M. F. S. (2014). Comparison of Human Ventral Frontal Cortex Areas for Cognitive Control and Language with Areas in Monkey Frontal Cortex. *Neuron*, *81*(3), 700–713. https://doi.org/10.1016/j.neuron.2013.11.012

Petrides, M., & Pandya, D. N. (1999). Dorsolateral prefrontal cortex: Comparative cytoarchitectonic analysis in the human and the macaque brain and

corticocortical connection patterns. *European Journal of Neuroscience*, *11*(3), 1011–1036. https://doi.org/10.1046/j.1460-9568.1999.00518.x

Phaf, R. H., Mohr, S. E., Rotteveel, M., & Wicherts, J. M. (2014). Approach, avoidance, and affect: A meta-analysis of approach-avoidance tendencies in manual reaction time tasks. *Frontiers in Psychology*, *5*. https://www.frontiersin.org/articles/10.3389/fpsyg.2014.00378

Polanía, R., Nitsche, M. A., Korman, C., Batsikadze, G., & Paulus, W. (2012). The Importance of Timing in Segregated Theta Phase-Coupling for Cognitive Performance. *Current Biology*, *22*(14), 1314–1318. https://doi.org/10.1016/j.cub.2012.05.021

Preisig, B. C., Riecke, L., Sjerps, M. J., Kösem, A., Kop, B. R., Bramson, B., Hagoort, P., & Hervais-Adelman, A. (2021). Selective modulation of interhemispheric connectivity by transcranial alternating current stimulation influences binaural integration. *Proceedings of the National Academy of Sciences*, *118*(7), e2015488118. https://doi.org/10.1073/pnas.2015488118

Reinhart, R. M. G., & Nguyen, J. A. (2019). Working memory revived in older adults by synchronizing rhythmic brain circuits. *Nature Neuroscience*, *22*(5), Article 5. https://doi.org/10.1038/s41593-019-0371-x

Roelofs, K., Minelli, A., Mars, R. B., van Peer, J., & Toni, I. (2009). On the neural control of social emotional behavior. *Social Cognitive and Affective Neuroscience*, *4*(1), 50–58. https://doi.org/10.1093/scan/nsn036

Roelofs, K., van Peer, J., Berretty, E., Jong, P. de, Spinhoven, P., & Elzinga, B. M. (2009). Hypothalamus–Pituitary–Adrenal Axis Hyperresponsiveness Is Associated with Increased Social Avoidance Behavior in Social Phobia.

Biological Psychiatry, *65*(4), 336–343. https://doi.org/10.1016/j.biopsych.2008.08.022

Ruhnau, P., Neuling, T., Fuscá, M., Herrmann, C. S., Demarchi, G., & Weisz, N. (2016). Eyes wide shut: Transcranial alternating current stimulation drives alpha rhythm in a state dependent manner. *Scientific Reports*, *6*(1), Article 1. https://doi.org/10.1038/srep27138

Saturnino, G. B., Madsen, K. H., Siebner, H. R., & Thielscher, A. (2017). How to target inter-regional phase synchronization with dual-site Transcranial Alternating Current Stimulation. *NeuroImage*, *163*, 68–80. https://doi.org/10.1016/j.neuroimage.2017.09.024

Scheeringa, R., Fries, P., Petersson, K.-M., Oostenveld, R., Grothe, I., Norris, D. G., Hagoort, P., & Bastiaansen, M. C. M. (2011). Neuronal Dynamics Underlying High- and Low-Frequency EEG Oscillations Contribute Independently to the Human BOLD Signal. *Neuron*, *69*(3), 572–583. https://doi.org/10.1016/j.neuron.2010.11.044

Schutter, D. J. L. G. (2016). Cutaneous retinal activation and neural entrainment in transcranial alternating current stimulation: A systematic review. *NeuroImage*, *140*, 83–88. https://doi.org/10.1016/j.neuroimage.2015.09.067

Schweizer, S., Grahn, J., Hampshire, A., Mobbs, D., & Dalgleish, T. (2013). Training the Emotional Brain: Improving Affective Control through Emotional Working Memory Training. *Journal of Neuroscience*, *33*(12), 5301–5311. https://doi.org/10.1523/JNEUROSCI.2593-12.2013

Thielscher, A., Antunes, A., & Saturnino, G. B. (2015). Field modeling for transcranial magnetic stimulation: A useful tool to understand the physiological effects of TMS? *2015 37th Annual International Conference of the IEEE Engineering in*

Medicine and Biology Society (EMBC), 222–225. https://doi.org/10.1109/EMBC.2015.7318340

van Peer, J. M., Spinhoven, P., Dijk, J. G. van, & Roelofs, K. (2009). Cortisol-induced enhancement of emotional face processing in social phobia depends on symptom severity and motivational context. *Biological Psychology*, *81*(2), 123–130. https://doi.org/10.1016/j.biopsycho.2009.03.006

Violante, I. R., Li, L. M., Carmichael, D. W., Lorenz, R., Leech, R., Hampshire, A., Rothwell, J. C., & Sharp, D. J. (2017). Externally induced frontoparietal synchronization modulates network dynamics and enhances working memory performance. *ELife*, *6*, e22001. https://doi.org/10.7554/eLife.22001

Volman, I., Roelofs, K., Koch, S., Verhagen, L., & Toni, I. (2011). Anterior Prefrontal Cortex Inhibition Impairs Control over Social Emotional Actions. *Current Biology*, *21*(20), 1766–1770. https://doi.org/10.1016/j.cub.2011.08.050

Voytek, B., Kayser, A. S., Badre, D., Fegen, D., Chang, E. F., Crone, N. E., Parvizi, J., Knight, R. T., & D'Esposito, M. (2015). Oscillatory dynamics coordinating human frontal networks in support of goal maintenance. *Nature Neuroscience*, *18*(9), Article 9. https://doi.org/10.1038/nn.4071

Wischnewski, M., Alekseichuk, I., & Opitz, A. (2023). Neurocognitive, physiological, and biophysical effects of transcranial alternating current stimulation. *Trends in Cognitive Sciences*, *27*(2), 189–205. https://doi.org/10.1016/j.tics.2022.11.013

Woolrich, M. W., Ripley, B. D., Brady, M., & Smith, S. M. (2001). Temporal Autocorrelation in Univariate Linear Modeling of FMRI Data. *NeuroImage*, *14*(6), 1370–1386. https://doi.org/10.1006/nimg.2001.0931